



EVALUATION OF THE HYDRAULIC CHARACTERISTICS OF FLOW OVER BROAD CRESTED WEIR BY USING ANSYS FLUENT

EVALUATION LES CARATERISTIQUES HYDRAULIQUE DE L'ÉCOULEMENT AU DESSUS D'UN DEVERSOIR Á PAROIS ÉPAISSE

BENTALHA C.

Department of Hydraulic Engineering, Abou Bekr Belkaid University, Tlemcen, Algeria

c_bentalha@yahoo.fr

ABSTRACT

Broad-crested weir is structure designed to measure the flow rates and to control the flood water in open channel. In the present numerical study, the Reynolds-Averaged Navier–Stokes equations are coupled with $k-\varepsilon$ turbulence standard model to simulate the water flow over broad-crested weir by using the software Ansys Fluent. Volume of fluid (VOF) model is used as a tool to track the free surface flow. This research aims to find new formulas for calculate the discharge coefficient (C_d) and to describe flow structure in the vicinity of backward broad crested. The found numerical results agree well with experimental results. The relative error between the measured and computed value of discharge coefficients does not exceed 2%. A very satisfactory agreement observed between numerical and experimental water surface profiles for different flow rates.

Keywords: Discharge coefficient, Broad-crested weir, Ansys Fluent, VOF Model, water surface profile, Standard $k-\varepsilon$ Model.

RÉSUMÉ

Le déversoir à seuil épais est un dispositif permettant de contrôler ou de mesurer le débit s'écoulant au-dessus de l'ouvrage. Il est plus adapté aux grands débits comparé à un déversoir à paroi mince. Dans cette étude numérique, les

équations de Reynolds sont couplées avec le modèle de turbulence $k-\varepsilon$ pour simuler l'écoulement de l'eau au-dessus d'un déversoir à parois épaisses en utilisant le code de calcul Ansys Fluent. Le modèle multiphasique VOF (Volume Of Fluid) est utilisé comme outil pour modéliser l'interaction eau-air près de la surface libre. Cette recherche vise à trouver de nouvelles formules pour calculer le coefficient du débit (C_d) et décrire la structure de l'écoulement au voisinage du déversoir à seuil épais. Les résultats trouvés numériquement sont en bon accord avec les résultats expérimentaux. L'erreur relative entre le coefficient du débit mesurés et calculés n'a pas dépassé 2%. Une très bonne concordance trouvée entre le profil de la surface libre mesuré et simulé.

Mots clés : coefficient du débit, déversoir à seuil épais, Ansys Fluent, méthode VOF, la surface libre, modèle ($k-\varepsilon$).

INTRODUCTION

Broad-crested weir is structure designed to measure the flow rates and to control the flood water in open channel. It is more suitable for large discharges when it's compared by sharp-crested weir. A broad-crested weir is a flat-crested structure with a length larger than the flow thickness (Figure 1). The ratio of crest length to upstream head over crest must be typically greater than 1.5–3 (Chanson, 2004):

$$\frac{L}{H_1} > 1.5 - 3 \quad (1)$$

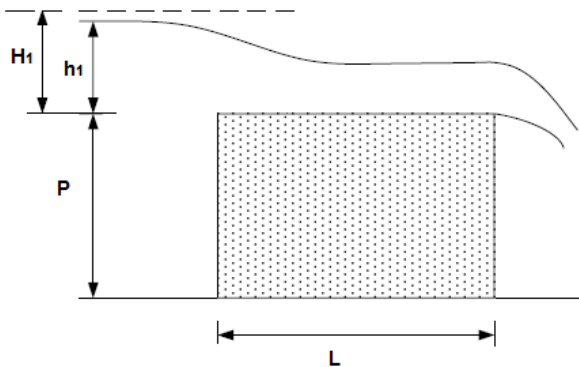


Figure 1: Flow pattern above a broad-crested weir

The flow streamline on broad-crest is parallel to the crest and the pressure distribution is hydrostatic (Felder and Chanson, 2012). For broad-crested weir, it is usually assumed that the flow will be critical on the weir crest.

Many researchers have studied the flow characteristics over broad crested weir. Bazin (1898) was the first to investigate on discharge capacity of broad crested weir. Horton (1907) suggested from the experiment that the discharge coefficient depends of ration H_1/L . Hager and Schwalt (1994) and Bos (1985) proposed an approach to estimate the discharge coefficient. Fritz and Hager (1998) found that the capacity of 1:2 sloping embankments is 15% larger than the standard broad-crested weir. They discussed also the flow regimes in terms of submergence and described the velocity distribution in arbitrary sections of the tailwater region. Azimi and Rajaratnam (2009) analyzed and developed useful correlations for the discharge coefficient in the general broad-crested weir equation. The experimental study of Goodarzi et al (2012) showed the effect of changing upstream slope of rectangular broad-crested weirs on discharge coefficient, velocity profile, and the flow separation zone. Felder and Chanson (2012) conducted an extensive series of experiments for calculating free-surface profiles, pressure and velocity distributions on a horizontal broad-crested weir with a rounded corner. Achour et al (2002) proposed theoretical approach to study the hydraulic jump controlled by sharp and broad-crested weirs.

Based on continuity and Bernoulli equations, the flow rate on the broad-crested weir is given by the following formula (Henderson, 1966):

$$Q = C_d \sqrt{g} b \left(\frac{2}{3} H_1 \right)^{3/2} = C_d 1.705 b H_1^{3/2} \quad (2)$$

Where:

H_1 = Total energy head (m) of upstream flow measured relative to the weir-crest elevation:

$$H_1 = h_1 + \frac{V_1^2}{2g} \quad (3)$$

h_1 = Upstream head relative to the top of the broad-crested weir (m).

V_1 = Approach velocity

Q = flowrate (m^3/s)

g = Gravity (m/s^2)

b = Breadth of weir (m).

C_d = Dimensionless discharge coefficient

In real application it is more convenient to use h_1 in the equation (2) instead of H_1 because the upstream velocity of approach can be neglected (Terry, 2001, Manson, 2009), hence, equation (2) can be expressed as

$$Q = C_d \sqrt{g} b \left(\frac{2}{3} h_1 \right)^{3/2} = C_d 1.705 b h_1^{3/2} \quad (4)$$

The discharge coefficient (C_d) is a function of the upstream sill-referenced energy head (H_1), the length and height of the weir crest in the direction of flow (L). It can be expressed by the equation (Bos 1985):

$$C_d = 0.93 + 0.1 \frac{H_1}{L} \quad (5)$$

Hager and Schwalt (1994) also derived a mathematical formula enabling the determination C_d :

$$C_d = 0.85 \frac{9}{7} \left(1 - \frac{2/9}{1 + (H_1/L)^4} \right) \text{ for } 0.1 < \frac{H_1}{L} < 1.5 \quad (6)$$

Currently, with the development of computational fluid dynamics (CFD) branch, flow over broad crested weir can be simulated to validate experimental results. Sarker and Rhodes (2004) used FLUENT commercial software for comparing numerical and measurement of the water surface profile. Hargreaves et al (2007) proved the capability of commercial CFD software to predict the important flow variables over a broad-crested weir. They used volume of fluid (VOF) to simulate interaction between air and water and turbulence was encountered by RNG k- ϵ . Haun et al (2011) tested two CFD codes; Flow-3D and SSIM 2 to simulate the water flow over trapezoidal broad crested weir. They found that Flow-3D required less time than SSIM 2. Amara and Berreksi (2018) used finite element method for the integration of the nonlinear differential equation of the side weir flow in rectangular channel. Numerical study of Reza et al. (2013) was performed to simulate and investigate flow characteristics over porous broad crested weirs. They employed three variants of the k- ϵ and the RSM models to find the water level and velocity distribution.

In this study, water flow over broad crested weir was simulated by using FLUENT software and VOF model was employed to define the free surface profile. Experimental results conducted by Goodarzi et al (2012) are the basis of comparison and validation in this work. They used a horizontal rectangular channel that was 12 m long, 0.25 m wide, and 0.5 m tall and tested eight different broad-crested weir configurations with various upstream slopes. Only one configuration of broad crested weir with slopes of 1V to 1H was analyzed

in this manuscript. The purpose of this study is to develop new relationships for determining the dimensionless discharge coefficient. In addition, to show the distribution of velocity and to study the characteristics of separated region flow.

NUMERICAL MODEL

Ansys Fluent computational fluid dynamics (2014) is used to solve the Reynolds-Averaged Navier-Stokes equations are based on momentum and mass conservation of multi-phase flow over stepped spillway. The standard k – ε turbulence model is adopted to enclose the equations.

Continuity equation:

$$\frac{\partial \rho}{\partial t} + \frac{\partial \rho u_i}{\partial x_i} = 0 \quad (7)$$

Momentum equation:

$$\frac{\partial \rho u_i}{\partial t} + \frac{\partial}{\partial x_j} (\rho u_i u_j) = -\frac{\partial p}{\partial x_i} + \rho g_i + \frac{\partial}{\partial x_j} \left\{ (\mu + \mu_t) \left(\frac{\partial u_i}{\partial x_j} + \frac{\partial u_j}{\partial x_i} \right) \right\} \quad (8)$$

Turbulence kinetic energy equation (k):

$$\frac{\partial}{\partial t} (\rho k) + \frac{\partial}{\partial x_i} (\rho k u_i) = \frac{\partial}{\partial x_j} \left[\left(\mu + \frac{\mu_t}{\sigma_k} \right) \frac{\partial k}{\partial x_i} \right] + G_k - \rho \varepsilon \quad (9)$$

Turbulence dissipation rate energy equation (ε):

$$\frac{\partial}{\partial t} (\rho \varepsilon) + \frac{\partial}{\partial x_i} (\rho \varepsilon u_i) = \frac{\partial}{\partial x_j} \left[\left(\mu + \frac{\mu_t}{\sigma_\varepsilon} \right) \frac{\partial \varepsilon}{\partial x_i} \right] + C_{\varepsilon 1} \frac{\varepsilon}{k} G_k - C_{\varepsilon 2} \rho \frac{\varepsilon^2}{k} \quad (10)$$

Where, G_k is production of turbulent kinetic energy which can be given as

$$G_k = \mu_t \left(\frac{\partial u_i}{\partial x_j} + \frac{\partial u_j}{\partial x_i} \right) \frac{\partial u_i}{\partial x_j} \quad (11)$$

μ_t is the turbulent viscosity that satisfies

$$\mu_t = \rho C_\mu \frac{k^2}{\varepsilon} \quad (12)$$

$C_\mu=0.09$ is a constant determined experimentally;

σ_k and σ_ε are turbulence Prandtl numbers for k and ε equation respectively, $\sigma_k=1.0$, $\sigma_\varepsilon=1.3$,

$C_{\varepsilon 1}$ and $C_{\varepsilon 2}$ are ε equation constants, $C_{\varepsilon 1}=1.44$, $C_{\varepsilon 2}=1.92$.

The volume of fluid (VOF) method is applied to simulate the free surface between water and air (Ansys Fluent 2014). In this approach, the tracking interface between air and water is accomplished by the solution of a continuity equation for the volume fraction of water:

$$\frac{\partial \alpha_w}{\partial t} + \frac{\partial \alpha_w u_i}{\partial x_i} = 0 ; 0 \leq \alpha_w \leq 1 \quad (13)$$

Where, α_w is volume fraction of water.

In each cell, the sum of the volume fractions of air and water is unity. So, volume fractions of air denote α_a can be given as

$$\alpha_a = 1 - \alpha_w \quad (14)$$

The volume fraction, momentum and turbulence closure equations were discretised by employing a conservative, second-order accurate upwind scheme. The pressure-velocity coupling algorithm is the pressure-implicit with splitting of operators (PISO). The boundary conditions in this study are velocity inlet as water inlet and air inlet, outlet as a pressure outlet type. All of the walls as a stationary, no-slip wall. The viscosity layer near to the wall dealt with the standard wall function (see figure 2).

The geometry of numerical model and boundary conditions are shown in figure 2. The three-dimensional numerical domain was divided into structured grids with 102609 hexahedral cells.

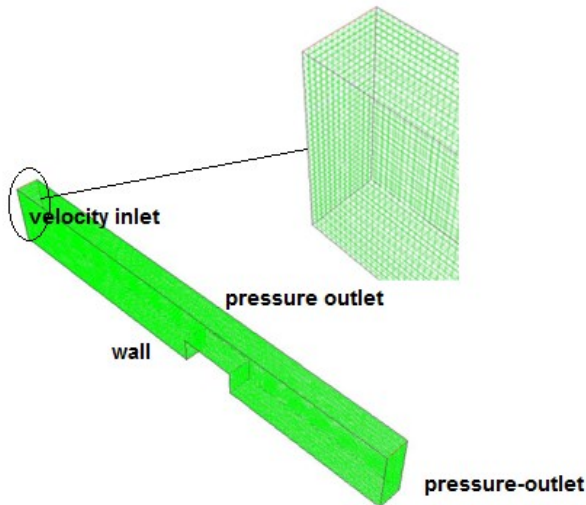


Figure 2: Boundary conditions and numerical model of a broad crested weir

RESULTS AND DISCUSSIONS

Among the objectives of this research is to validate the experimental data of Cd and to develop other correlation for this parameter. Table 3 shows the measured and computed value of discharge coefficients and flow rate obtained by Ansys Fluent. The numerical results were very close to experimental because the relative error between 0.28 and 2 %.

After analyzing the experimental and numerical results, new relationships was developed. The advantage of these formulas are depends of water depth above broad crested weir (h_1) and not of total energy head (H_1), which means that the calculation of velocity approach (V_1) is neglected. A linear fit as provided in equation (15) and it's plotted in figure (3). This figure indicates that the dimensionless discharge was best fitted by this correlation:

$$Cd = 0.825 + 0.34 \left(\frac{h_1}{L} \right) \quad (15)$$

Table 1: Computed and measured coefficient discharge

Q_{exp}	Q_{CFD}	Cd_{exp}	Cd_{CFD}	Relative error(%)
0.035	0.0351	0.9364	0.9391	0.28
0.03	0.0306	0.9195	0.9379	2
0.025	0.0254	0.9089	0.9234	1.6
0.02	0.0201	0.8971	0.9015	0.5
0.015	0.0153	0.8859	0.9036	2

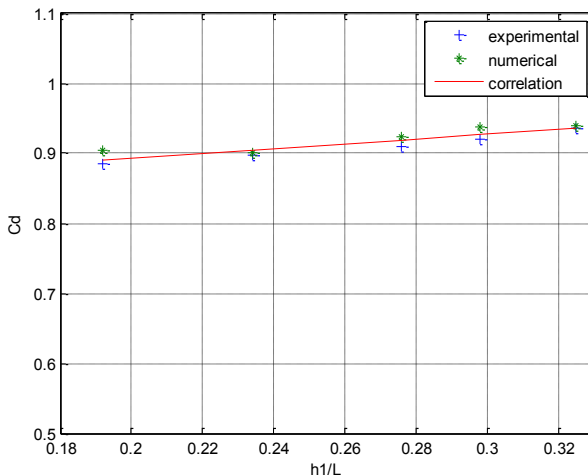


Figure 3 : Numerical and experimental Cd compared with equation (15)

In order to include more characteristics geometric of broad crested weir in regression analysis of results, the height of crest (P) was added in this analysis and it's presented in equation (16). A comparison of equation (16) to experimental and numerical data of Cd proves to be well method for evaluating coefficient discharge (see figure 4)

$$Cd = 0.66 + 0.36 \left(\frac{h_1+P}{L} \right) \tag{16}$$

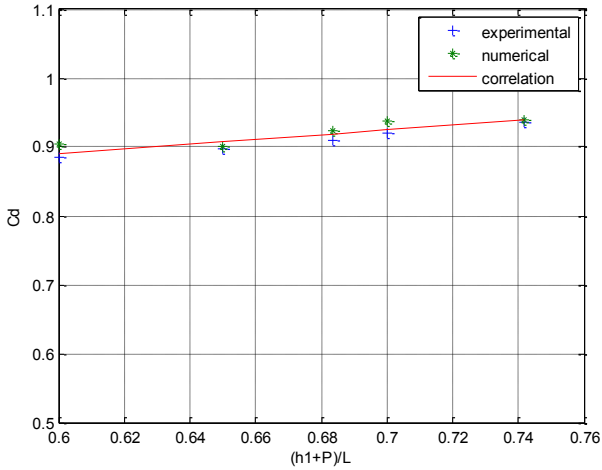


Figure 4: Numerical and experimental Cd compared with equation (16)

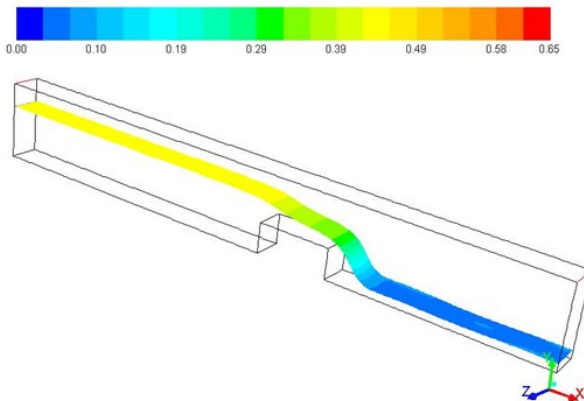


Figure 5: Y-coordinate of free surface profile in channel for $Q= 0.035 \text{ m}^3/\text{s}$.

Figure 5 shows 3D- free surface profile in a horizontal rectangular flume equipped by broad crested weir. This figure indicate that the flow upstream is subcritical, accelerates to critical near the top of the weir, and spills over into a supercritical nappe.

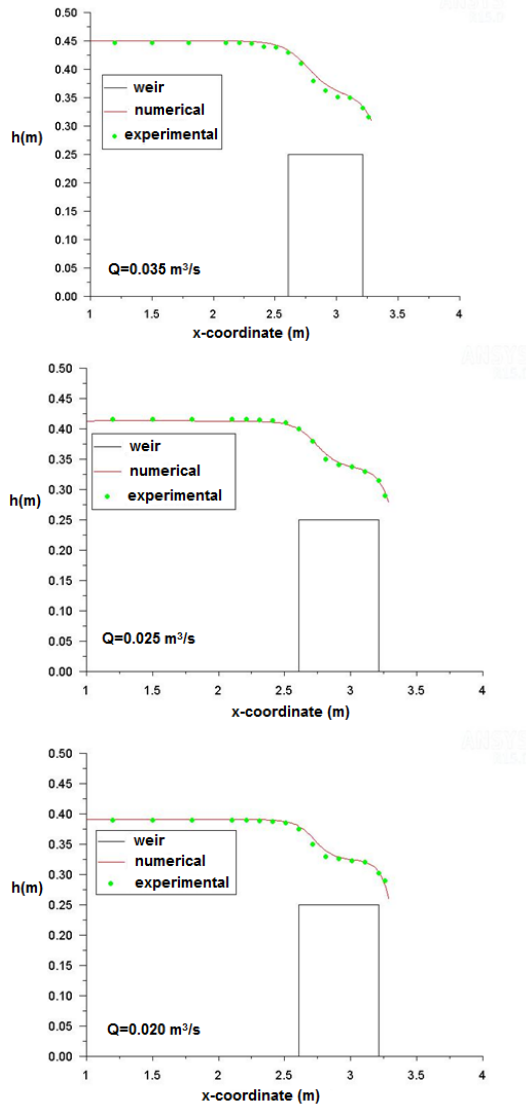


Figure 6: Comparison between numerical and experimental water surface profile

Figure 6 compares numerical and experimental water surface profiles for different flow rates. A very satisfactory agreement can be observed between both results. This figure proved that the VOF model is an excellent tool to predict water surface profile.

Figure 7 show the velocity distribution predicted by Ansys Fluent. This figure indicate that the velocity of flow upstream is very low and increased above the broad crested weir to attain critical velocity after the flow downstream becomes supercritical. The vortex zone with returning velocity vectors was developed in the right corner of weir. Due the sudden expansion, the strong recirculation flow produces in the right corner of weir. The returning velocity vectors increased near the bed where the viscosity force is dominant.

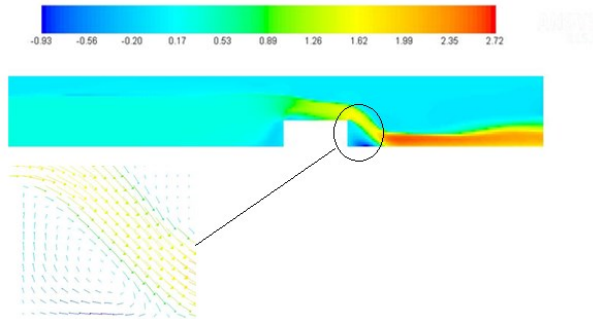


Figure 7 : Contour of velocity over broad crested weir for $Q= 0.035 \text{ m}^3/\text{s}$.

The size of the recirculation zone increases with increasing of flow rate because the negative pressure is more developed for high velocity (figure 8). At the distance "Ls" called the reattachment length, the flow resumes in the positive flow direction all over the cross-section. Based on the study of Armaly et al (1983) and Hung Le et al (1997), the reattachment length depend of Reynolds number based on the expansion height and the flow geometries. In open channel flow with a backward step, Nakagawa and Nezu (1987) found that the recirculation length tends to increase gradually with increasing Froude number. In this paper, the reattachment length of the separated flow are investigated with Reynolds number based on the critical velocity and height of broad crested weir:

$$Re_c = \frac{V_c P}{\nu}$$

where V_c is critical velocity, P height of broad crested weir and ν is kinematic viscosity.

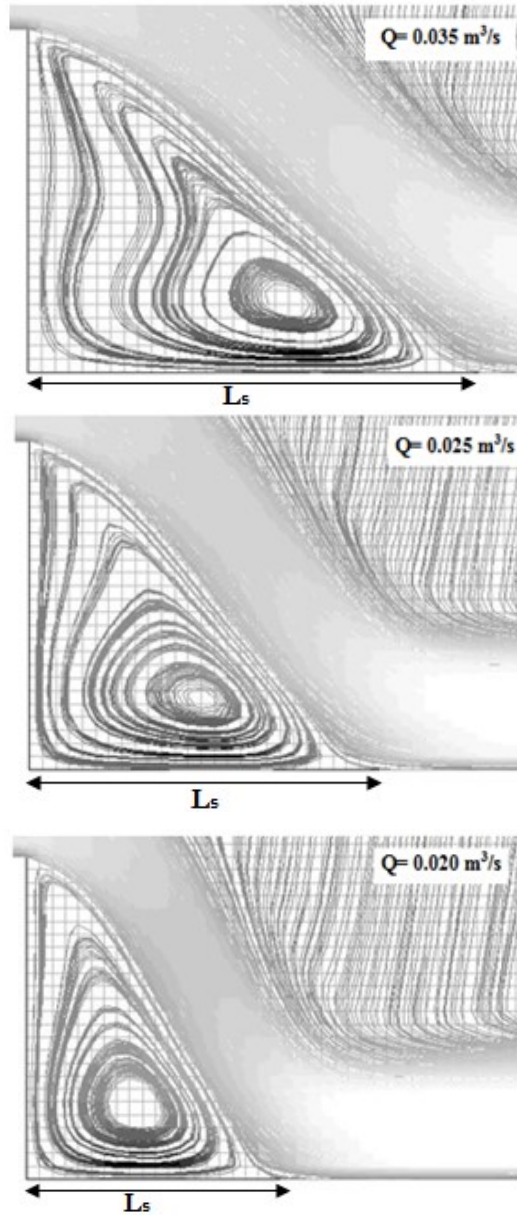


Figure 8: Streamlines in the vicinity of backward broad crested for different flow rate

Figure 9 display the variation of reattachment length normalized by height of broad crested weir with Reynolds number. This figure illustrated that with increasing Reynolds number, the reattachment length increases. The profile of normalized reattachment length was best fitted by the following equations:

$$\frac{L_s}{P} = 3.52 \ln(Re_c) - 2.1 \tag{17}$$

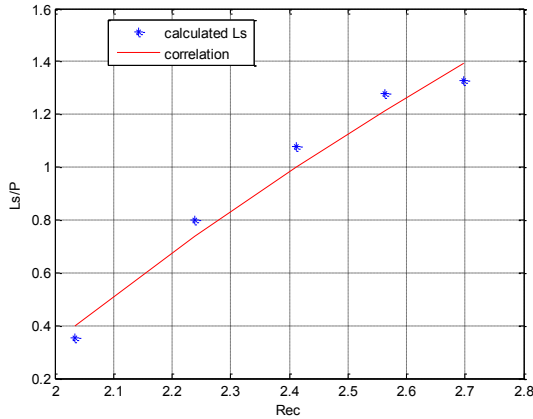


Figure 9 : Variation of reattachment length with Reynolds number

CONCLUSION

A numerical study was performed to investigate flow over broad crested weir by using Ansys Fluent. Free surface was treated by VOF model and turbulence flow was estimated by $k - \epsilon$ Standard Model. Good agreement is found between numerical and experimental results. The relative error between measured and calculated coefficient discharge less than 2%. These results was best correlated by equation (15) and (16).The advantage of these formulas lies in the fact that discharge coefficient depends of water depth above broad crested weir and not of total energy head.

The magnitudes of longitudinal of velocity increased along the broad crested weir and the vortex zone with returning velocity vectors was developed in the right corner of weir. It was found that by increasing of flow rate, the size of the recirculation zone increased. The profile of normalized reattachment length was best presented by a logarithmic regression model equation (equation17).

REFERENCES

- ACHOUR B., SEDIRA N., M. DEBABECHE M., (2002). Ressaut contrôlé par seuil dans un canal rectangulaire. Larhyss Journal, n° 1, pp.73-85.
- AMARA L., BERREKSI A., (2018). Computation of 1d side weir flow by finite element method. Larhyss Journal, n° 35, pp. 45-58.
- ANSYS Inc. (2014). ANSYS Fluent Version 15.0.7 User's Guide.
- ARMALY B., DURST F., PEIREIRA J.C.F., SCHÖNUNG B., (1983). Experimental and theoretical investigation of backward-facing step flow. Journal of Fluid Mechanics Vol 127, pp.473–496.
- AZIMI A. H., RAJARATNAM N., (2009). Discharge characteristics of weirs of finite crest length, Journal of Hydraulic Engineering, Vol. 135, Issue 12, pp.1081–1085.
- BAZIN H., (1896). Expériences Nouvelles sur l'Écoulement par Déversoir. Recent experiments on the flow of water over weirs. (In French) Mémoires et Documents, Annales des Ponts et Chaussées, Série 7, Vol. 12, 2 semestre, pp.645–731. (referenced in Felder and Chanson 2012).
- BOS M. G., (1985). Broad-crested weirs and long-throated flume. Martinus Nijhoff, Dordrecht, The Netherlands, 141p.
- CHANSON.H (2004) .The Hydraulics of Open Channel Flow: An Introduction. Butterworth-Heinemann. ISBN: 9780750659789, 650p.
- FELDER S., CHANSON H. (2012). Free-surface Profiles, Velocity and Pressure Distributions on a Broad-Crested Weir: a Physical study. Journal of Irrigation and Drainage Engineering, ASCE, Vol.138, Issue 12, pp.1068–1074.
- FRITZ H. M., HAGER H. W., (1998): Hydraulics of Embankment Weirs. Journal of Hydraulic Engineering, ASCE., Vol. 124, Issue 9, pp.963–971.
- GOODARZI E., FARHOUDI J., SHOKRI N., (2012). Flow Characteristics of Rectangular Broad-Crested Weirs with Sloped Upstream Face. Journal of Hydrology and Hydromechanics, Vol. 60, Issue 2, pp.87–100.
- HAGER, H. W., SCHWALT M., (1994). Broad-crested weir. Journal of Irrigation and Drainage Engineering., Vol. 120, Issue 1, pp.13-26.
- HARGREAVES D., MORVAN H., WRIGHT N., (2007). Validation of the volume of fluid method for free surface calculation: The broad-crested weir. Engineering. Application Computational Fluid Mechanics. Vol 1, Issue 2, pp.136–146.
- HAUN S., OLSEN N.R.B., FEURICH R.,(2011). Numeircal modeling of flow over trapezoidal broad crested weir. Journal of engineering application of computational fluid dynamics, Vol 5, Issue 3, pp.397-405

- HUNG L.E., PARVIZ M., JOHN K., (1997). Direct numerical simulation of turbulent flow over a backward-facing step. *Journal of Fluid Mechanics*. Vol. 330, Issue 1, pp.349-374
- HENDERSON F.M. (1966). *Open channel flow*. McMillan series in Civil Engineering, New York, 544p.
- HORTON, R. E. (1907). Weir experiments, coefficients, and formulas. Proc., U.S. Geological Survey Water Supply, Government Printing Office, Washington, DC.,235p.
- MUNSON B.R., YOUNG, D. F., THEODORE H.O., Wade W.H. (2009). "Fundamentals of Fluid Mechanics", John Wiley & Sons, Inc, Sixth Edition, ISBN 978-0470-26284-9, 783p.
- NAKAGAWA H., NEZU I. (1987).Experimental investigation on turbulent structure of backward-facing step flow in an open channel. *Journal of Hydraulic Research*, Vol. 25, n°1, pp.67-88.
- SARKER M.A., RHODES D.G. (2004).Calculation of free surface profile over a rectangular broad crested weir, *Flow measurement and instrumentation*, Vol 15,Issue 4, pp.215-219.
- TERRY W.S. (2001). *Open Channel Hydraulics*. Mc Graw-Hill Education, 560p, ISBN 0-07-120180-7.